Dissociation Mechanism of a Stable Intermediate: Perfluorohydroxylamine

Hasan Sayin and Michael L. McKee*

Department of Chemistry and Biochemistry, Auburn University, Auburn, Alabama 36849

Received: March 21, 2006; In Final Form: May 24, 2006

The mechanism of dissociation of F_2NOF has been studied using density-functional (B3LYP, BB1K, and MPWB1K) and wave function methods (CCSD). Variational transition state theory was used to calculate the rate constants for *cis*-$F_2NOF \rightarrow FNO + F_2$ (concerted), *cis*-$F_2NOF \rightarrow F_2NO + F$, and *cis*-$F_2NOF \rightarrow$ *trans*-$F_2NOF \rightarrow F_3NO$. Rate constants were also calculated for the dissociation of F_2NOF by using transition state theory. The enthalpies of the transitions states (CCSD(T)/cc-pVQZ//B3LYP/6-311+G(d)) were very close to the enthalpy of separated $F_2NO + F$ radicals which implies temperature-dependent competition between concerted rearrangement and fragmentation-recombination. The picture is further complicated by the fact that F_2NO undergoes fragmentation into $FNO + F$ with a very low barrier. Thus, formation of F_3NO, the global minimum on the potential energy surface, can only occur by a concerted process (not from $F_2NO + F$). The data were fit to a temperature-dependent rate in the range 200−1000 K in the form $k_2 = 8.14 \times 10^{13} \exp(-7860/T)\ s^{-1}$, $k_1 = 6.37 \times 10^{13} \exp(-7855/T)\ s^{-1}$, and $k_{10} = 1.42 \times 10^{12} \exp(-7420/T)$ for *cis*-$F_2NOF \rightarrow FNO + F_2$ (concerted), *cis*-$F_2NOF \rightarrow F_2NO + F$, and *cis*-$F_2NOF \rightarrow F_3NO$, respectively. The calculated lifetime of *cis*-F_2NOF at 298K is 2.5×10^{-3} s via k_1.

Introduction

Perfluorohydroxylamine, F_2NOF, is an interesting example of an electron rich molecule that may have a number of competitive rearrangement pathways. There are several theoretical studies reported for this molecule;[1,2] semiempirical,[3] Hartree−Fock methods,[4] and coupled cluster theory[1,2] which find that the cis conformation is more stable than trans. Although the structure, stability, and thermochemistry of this compound have not been investigated experimentally, Antoniotti et al.[1] suggested that F_2NOF is an intermediate in the reaction between $O(^1D)$ and NF_3 which produced F_2N and FO radicals and Bedzhanyan et al.[6] suggested that F_2NOF can be an intermediate in the $F_2N + FO$ reaction.

On the other hand, the F_3NO isomer has been structurally characterized and possesses a N−O bond with a high degree of double bond character ($r_{N-O} = 1.159$ Å).[5] Antoniotti and Grandinetti studied[1] the dissociation pathway of F_3NO at the CCSD(T)/aug-cc-pVTZ//CCSD/cc-pVDZ level and found a transition state for the rearrangement of *trans*-F_2NOF to F_3NO with a 22.1 kcal/mol enthalpy barrier. As discussed below, their transition state corresponds to a higher-lying structure with strong zwitterionic character. The true transition state has much higher biradical character. Bedzhanyan et al.[6] studied the reaction between F_2N and FO radicals and found the dominant channel to be eq 1.

$$F_2N + FO \rightarrow FNO + 2F \tag{1}$$

A reasonable mechanism would have the radicals associate to form F_2NOF which could then dissociate to $FNO + 2F$ through a stepwise cleavage of F atoms.

To our knowledge, the experimental vibrational spectra for F_2NOF has not been reported. Misochko et al.[7] measured the infrared absorption spectra and EPR spectra of the F_2NO radical at 20 K in an argon matrix, as well as infrared absorption spectra for FNO, F_2NO, and F_3NO, but did not identify F_2NOF. Although postulated as an intermediate in several reaction mechanisms, F_2NOF has not been identified experimentally.

A reasonable mechanism of F_2NOF dissociation would include eq 2−6.

$$F_2NOF \rightarrow F_2N + OF \tag{2}$$

$$F_2NOF \rightarrow FNO + F_2 \tag{3}$$

$$F_2NOF \rightarrow F_2NO + F^{\bullet} \tag{4}$$

$$F_2NO \rightarrow FNO + F^{\bullet} \tag{5}$$

$$F^{\bullet} + F^{\bullet} \rightarrow F_2 \tag{6}$$

Equation 4, the O−F dissociation step, has some similarities with O−X dissociations in ONO−X (X = F, Cl, Br, OH, and OCl). When X = F, Ellison et al.[8] showed that there is direct isomerization between *cis*-ONOF and FNO_2 with an activation energy of 22 ± 3 kcal/mol. When X = Cl, the *cis*-ONOCl → $ClNO_2$ transition state corresponds to fragmentation with a 20.9 kcal/mol barrier.[9] Kovačič et al.[10] recently calculated an isomerization path between *cis*-ONOBr and $BrNO_2$ with an activation barrier of 20.2 kcal/mol. On the other hand, when X = OH, the concerted formation of HNO_3 from HOONO is still not well established.[11] Zhao et al.[11a] showed that there is no direct isomerization between HOONO and $HONO_2$. On the other hand, a recent analysis using master equation simulation[11b] found that the best fit with experimental data occurs when the transition state for *trans*-HOONO → $HONO_2$ is 5.2 kcal/mol lower in energy than $HO + NO_2$. The O−O cleavage occurs from *cis*-HOONO with an activation barrier of 18−19 kcal/mol to form $NO_2 + OH$.

* To whom correspondence should be addressed. E-mail: mckee@chem.auburn.edu.

10.1021/jp061753w CCC: $33.50
Published on Web 08/24/2006

A similar mechanism of O−O cleavage occurs in the *cis*-ClOONO → $ClONO_2$ reaction with an activation energy of 28.4 and 6.7 kcal/mol from studies by Kovačič et al.[12] and Zhu et al.,[13] respectively.

Fox et al.[14] reported the synthesis of F_3NO from FNO plus F in a fluorine-nitric oxide flame. The authors suggested that fluorination of an excited state of F_2NO (formed in the 2000 K flame) might be involved in the mechanism.

In this paper, we will use theoretical methods to calculate the potential energy surface for the dissociation of the F_2NOF molecule and calculate the rate constant for formation of products over the temperature range 200−1000 K. All of the calculated rate constants reported below are at the high-pressure limit.

Computational Method

Density functional theory (DFT), widely used as a computational chemistry tool providing reasonable accuracy at modest computational cost, is used in this study because it has been shown to give reasonable structures and vibrational frequencies for halogen compounds.[15−18] We optimized geometries at the B3LYP/6-311+G(d) level, but we checked our results by reoptimizing with BB1K[19] and MPWB1K[20] which are hybrid meta DFT methods specifically designed to yield good results for kinetics. Beside the 6-311+G(d)[21] basis set, we also used the MG3S[22] basis set which is equivalent to 6-311+G(2df,2p) for systems without elements heavier than F. We also checked some of the stationary points with multiconfigurational SCF to determine the effect of adding additional configurations to the wave function. Last, we reoptimized most structures at the CCSD/6-31+G(d) level as a further check on consistency of prediction. Since the CCSD(T) method with a reasonable basis set yields very good results for different chemical systems such as O_3[23] and FOOF,[24] we based our kinetics calculations on energies at CCSD(T)/cc-pVQZ//B3LYP/6-311+G(d) unless indicated otherwise.

All electronic structure calculations have used the Gaussian 03[25] and Gamess[26] program systems. All imaginary frequencies for transition states were animated by using the graphical program MolDen[27] to make sure that the motion of the transition vector was appropriate for converting reactants to products.

The transition states involving bond formation or bond breaking were computed with an unrestricted method (UDFT or UHF) to determine the lower-energy spin broken-symmetry solution at the UDFT or UCCSD levels. Single-point calculations were made with a 16-electron 11-orbital complete active space[28] (CASSCF(16e,11o)) and the 6-311+G(d) basis set with dynamic electron correlation introduced at the MP2 level (MCQDPT2).[29] Optimization of radical fragments and most F_2-NOF stationary points were also carried out at the CASSCF-(16e,11o) level (Table 2 and Table S5). However, the transition states that were characterized by a loosely associated F atom (Abst-F_2−ts-c, Add-F−N-ts, and F_2−FON-ts) could not be located at the CASSCF level probably due to the lack of dynamic electron correlation in the CASSCF method. T1 diagnostics were computed at the CCSD level (Table 2) for several of the transition states. Values larger than 0.02 are often used as an indicator of significant multireference character. It is noteworthy that F_2NO−F-ts had a value of 0.02.

The intrinsic reaction coordinate[30] (IRC) is constructed starting from the saddle point geometry and going downhill to both the asymptotic reactant and product channels in mass-weighted Cartesian coordinates. Along each IRC, the reaction coordinate, *s*, is defined as the signed distance from the saddle point, with $s > 0$ referring to the product side. Once accurate approximations to the stationary points on the potential energy surface (PES) are available, reaction rate constants can be calculated using variational transition-state-theory (VTST).[31−33]

Three programs were used to compute rate constants. For reactions without a transition structure, Variflex-1.0[34] was used (k_1, k_5, k_6, and k_{11}, see below). For the conversion of *cis*-F_2-NOF to *trans*-F_2NOF, Chemrate-1.21[35] was used (k_3, see below). For other reactions with a transition state structure, Polyrate-9.3[36] was used either with conventional transition state theory (k_4, k_7, and k_8, see below) or with variational transition state theory (k_2, see below).

Results and Discussions

The calculated equilibrium structures of F_3NO are in good agreement with each other and with the experiment (Figure 1). The O−F bond distance of *cis*-F_2NOF has the largest sensitivity with respect to method, with CCSD(T)/6-311+G(d) giving the longest O−F bond distance and MPWB1K/MG3S the shortest. Likewise, there were large differences in the N−O bond of *cis*-F_2NOF with CCSD(T)/6-311+G(d) giving a short N−O bond distance and MPWB1K/MG3S giving a long N−O distance. The B3LYP DFT method made predictions in closest agreement with CCSD(T).

Table 1 shows the comparison of the calculated frequencies of *cis*-F_2NOF, *trans*-F_2NOF, and F_3NO. The calculated frequencies are in agreement with each other for *cis*-F_2NOF with slightly less agreement for the ONF bend (ω_5). For F_3NO, the calculated frequencies are in agreement with each other and very close to experimental results. It is interesting to point out that the CCSD-(T) method gave one imaginary frequencies for *trans*-F_2NOF with a small basis set (cc-pVDZ)[37] but all real frequencies with bigger basis sets (6-311+G(d) and 6-311+G(df)).

A lower-energy spin broken-symmetry solution was obtained at the UDFT and UCCSD levels in transition states involving bond formation or bond breaking (Table 2). We checked two of these transition states energies by using MCQDPT2/6-311+G(d)//UB3LYP/6-311+G(d).

The two bonds involving fluorine in the transition state (Abst-F_2–ts-*c*) for the reaction *cis*-F_2NOF → FNO + F_2 are very asymmetrical (Figure 2); one bond is almost completely broken (F−O 2.694 Å), whereas the other (F−N, 1.446 Å) shows no lengthening. Also, the newly forming F−F bond (2.557 Å) is very long. These factors led us to believe that the maximum along the PES might be sensitive to computational method. For these reasons, the rate constant was calculated with VTST using Polyrate. An intrinsic reaction coordinate (IRC) was calculated in mass-weighted coordinates at the B3LYP/6-311+G(d) level. At 10 points along the IRC, single-point energies were computed at the UCCSD(T)/cc-pVTZ, whereas a generalized normal-mode analysis was performed at the B3LYP/6-311+G(d) level projecting out the reaction coordinate. Despite expectations, the maximum at the UCCSD(T)/cc-pVTZ level occurred at a path value of $s = 0$, the same as the maximum at the B3LYP/6-311+G(d) level.

Because the spin broken-symmetry UCCSD(T)/cc-pVQZ calculations proved to be too lengthy, we estimated the relative energy of Abst-F_2-ts-*c* at the UCCSD(T)/cc-pVQZ level by taking the Abst-F_2-ts-*c*/F_2NO+F energy difference at the UCCSD(T)/cc-pVTZ level (0.72 kcal/mol more stable than radicals) and applying it to UCCSD(T)/cc-pVQZ relative energy of F_2NO + F.[38] The natural population analysis (NPA) at the UB3LYP/6-311+G(d) level showed that the loosely bound fluorine has nearly a full unpaired electron and has very little charge which means the transition state is biradical rather than zwitterionic.

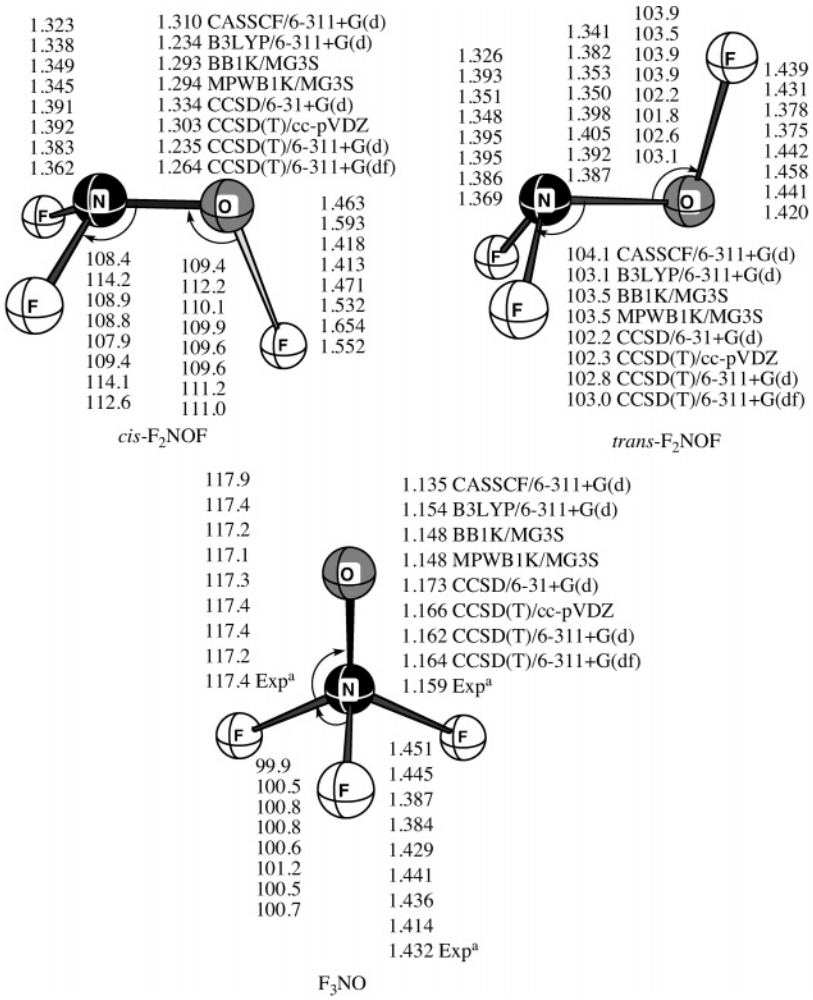

Figure 1. Optimized geometry of *cis*-F_2NOF, *trans*-F_2NOF, and F_3NO isomers. Bond lengths are in Å and angles are in degrees. For each isomer, methods are shown with the data. The last row in F_3NO isomers are experimental values. (a) Frost, D. C.; Herring, F. G; Mitchell, K. A. R; Stenhouse, I. R. *J. Am. Chem. Soc.* **1971**, *93*, 1596.

TABLE 1: Harmonic Frequencies of *cis*-F_2NOF, *trans*-F_2NOF, and F_3NO in cm^{-1}

method									
cis-F_2NOF	$\omega_1(a')$	$\omega_2(a'')$	$\omega_3(a')$	$\omega_4(a')$	$\omega_5(a'')$	$\omega_6(a')$	$\omega_7(a')$	$\omega_8(a')$	$\omega_9(a'')$
B3LYP/6-311+g(d)	1242	914	838	742	584	531	474	207	195
BB1K/MG3S	1150	1040	994	852	798	595	559	296	215
CCSD/6-31+G(d)	1065	975	895	823	733	549	518	277	196
CCSD(T)/cc-pVDZ	1046	910	850	750	556	547	474	232	194
CCSD(T)/6-311+G(d)	1230	951	827	696	578	518	346	189	113
CCSD(T)/6-311+G(df)	1181	1023	887	748	589	533	385	204	101
trans-F_2NOF	$\omega_1(a')$	$\omega_2(a')$	$\omega_3(a'')$	$\omega_4(a')$	$\omega_5(a')$	$\omega_6(a')$	$\omega_7(a'')$	$\omega_8(a')$	$\omega_9(a'')$
B3LYP/6-311+G(d)	1031	937	866	733	597	474	463	394	53
BB1K/MG3S	1144	1084	1029	941	668	518	512	431	63
CCSD/6-31+G(d)	1058	967	957	876	612	477	471	395	−28
CCSD(T)cc-pVDZ	1007	883	878	764	586	465	460	384	−19
CCSD(T)/6-311+G(d)	1028	910	897	797	596	473	467	391	40
CCSD(T)/6-311+G(df)	1073	968	951	849	627	489	477	401	43
F_3NO	$\omega_1(a_1)$	$\omega_2(e)$	$\omega_3(e)$	$\omega_4(a_1)$	$\omega_5(a_1)$	$\omega_6(e)$	$\omega_7(e)$	$\omega_8(e)$	$\omega_9(e)$
B3LYP/6-311+G(d)	1787	881	881	758	533	520	520	393	393
BB1K/MG3S	1785	974	974	857	609	602	602	438	438
CCSD/6-31+G(d)	1735	936	936	788	561	560	560	406	406
CCSD(T)/cc-pVDZ	1790	899	899	729	534	514	514	397	397
CCSD(T)/6-311+G(d)	1764	896	895	742	541	522	522	402	402
CCSD(T)/6-311+G(df)	1741	932	932	785	573	556	556	415	415
exp[a]	1852	874		741		529		403	

[a] Smardzewski, R. R.; Fox, W. B. *J. Chem. Phys.* **1974**, *60*, 2193.

Unlike the reaction *cis*-$F_2NOF \rightarrow FNO + F_2$, the transition state ($F_2NOF$-ts) in the *cis*-$F_2NOF \rightarrow$ *trans*-F_2NOF isomerization did not involve bond forming or breaking, only the rotation of OF about the N−O bond which was about mid-way between

TABLE 2: Relative Enthalpies[a] (kcal/mol) for Various Species Involved in the Dissociation of F_2NOF Molecule

					//B3LYP/6-311+G(d)[b]			
	BB1K/ MG3S	MPWB1K/ MG3S	CCSD/ 6-31+G(d)	MCQDPT2/ 6-311+G(d)[b,c]	B3LYP/ 6-311+G(d)	MCQDPT2/ 6-311+G(d)	CCSD(T)/ cc-pVTZ[d]	CCSD(T)/ cc-pVQZ[d]
cis-F_2NOF	0.00	0.00	0.00	0.00	0.00	0.00	0.00	0.00
trans-F_2NOF	5.89	5.84	4.51	10.76	9.06	9.36	3.80	4.31
F_3NO	−35.38	−35.36	−28.55	−39.80	−33.98	−33.44	−34.07	−34.63
Abst-F_2-ts-*c*[e]	10.98				8.94	12.05	13.80(0.07)	[15.25][g]
Add-F−N-ts	27.06	27.69	34.01		21.27	36.06	29.77(0.04)	27.37
F_2NO−F-ts[e]	17.15	17.44	18.57	17.31	13.90	15.66	14.11(0.02)	14.10(0.02)
F_2NOF-ts	14.06	14.05	12.37	11.01	16.13	15.35	10.91	11.31
F−F_2NO-ts[e]				7.73[f]	9.54	1.67	14.25(0.08)	[14.51][h]
F_2−FON-ts[e]					18.92	12.27	23.00(0.04)	[24.45][g]
complex[e]				8.17	7.56	8.44	16.54(0.04)	[9.89][h]
F_2NO + F	9.48	10.13	9.12	14.76	10.45	8.23	14.52	15.97
FNO + F_2	−7.79	−6.30	−17.56	−8.23	−10.73	−11.64	−16.46	−15.55
FNO + 2F				16.52	20.48	24.33	17.74	20.54
F_2N + OF	33.78	34.73	29.41	50.16	35.24	36.03	35.57	38.16
NO + 3F					79.12		71.12	81.98

[a] Thermodynamic corrections to produce enthalpies at 298 K are made from frequencies computed at the given level except where indicated. [b] Thermodynamic corrections are made at the B3LYP/6-311+G(d) level. [c] Geometries are optimized at the CASSCF(16e,11o)/6-311+G(d) level. [d] T1 diagnostic at the CCSD level is given in parentheses. [e] Geometries are optimized at the UDFT and UCCSD level. Spin-squared $\langle S^2\rangle$ values at UB3LYP/6-311+G(d) are 0.93, 0.13, 0.93 0.95 and 0.80 for Abst-F_2-ts-*c*, F_2NO−F-ts, F−F_2NO-ts, F_2−FON-ts, and complex, respectively. [f] Did not fully meet optimization criterion. [g] The energy at the CCSD(T)/cc-pVQZ level is estimated by taking the energy difference with F_2NO + F at the CCSD(T)/cc-pVTZ level and adjusting to the CCSD(T)/cc-pVQZ energy of F_2NO + F (15.97 kcal/mol). [h] The effect of spin contamination was projected out of the B3LYP/6-311+G(d) energies using the formula $E_{singlet} = (2E_{BS} - \langle S^2\rangle \cdot E_{triplet})/(2 - \langle S^2\rangle)$, where $\langle S^2\rangle$ is the spin-squared value of the singlet broken-symmetry solution (E_{BS}) and $E_{triplet}$ is the energy of the triplet at the singlet geometry. In addition, the "corrected" energy difference between "F−F_2NO-ts" or "complex" and F_2NO + F at the B3LYP/6-311+G(d) level is subtracted from the CCSD(T)/cc-pVQZ relative energy of F_2NO + F (15.97 kcal/mol).

cis (0°) and trans (180°). Therefore, we felt that the position of the transition state was probably not sensitive to method, and we used normal transition state theory with Chemrate. The calculated enthalpy barrier at the CCSD(T)/cc-pVQZ//B3LYP/6-311+G(d) level was 11.31 kcal/mol which is slightly less than the barrier for the *cis*-$F_2NOF \rightarrow FNO + F_2$ reaction (15.25 kcal/mol, Table 2).

The transition state (F_2NO−F-ts) in *trans*-$F_2NOF \rightarrow F_3NO$ was found at the UB3LYP/6-311+G(d), UBB1K/MG3S, UMPWB1K/MG3S, and UCCSD/6-31+G(d) levels. The O···F calculated distance in the transition state (Figure 2, F_2NO−F-ts) is rather short (1.643 Å, UB3LYP/6-311+G(d)). Ellison et al.[8] also found similar short O···F distances of 1.726 and 1.693 Å in the *trans*-$ONOF \rightarrow FNO_2$ transition state at the RCCSD(T) and UCCSD(T)/cc-pVTZ levels, respectively. A similar tight transition state is obtained for O−Cl cleavage in our previous study[9] of *trans*-$ONOCl \rightarrow ClNO_2$ where a O···Cl distance of 2.191 and 2.067 Å was calculated in the transition state at the RCCSD(T) and UCCSD(T)/cc-pVDZ levels, respectively.

Since little spin contamination was found at the UB3LYP/6-311+G(d) level (F_2NO−F-ts, $\langle S^2\rangle = 0.13$), restricted CCSD (RCCSD(T)/cc-pVQZ) was used rather than unrestricted CCSD. The enthalpy (298 K) of the transition state is 1.87 kcal/mol lower than F_2NO + F which implies the product is a complex rather than free radicals. We located a complex with a spin-squared value ($\langle S^2\rangle = 0.80$) which was 3.45 kcal/mol lower in enthalpy (298K) than F_2NO−F-ts and 2.89 kcal/mol lower than F_2NO + F at the B3LYP/6-311+G(d) level. The O−F bond increased from 1.643 Å in the transition state (F_2NO−F-ts) to 2.086 Å in the complex. From the complex, a second transition state (F−F_2NO-ts) was reached with an enthalpy of activation of 1.98 kcal/mol and a spin-squared value of 0.93 at the B3LYP/6-311+G(d) level. At the DFT level, the description of the $F_2NOF \rightarrow F_3NO$ reaction is stepwise via a shallow intermediate which is concerted in the sense that the same fluorine that leaves oxygen adds to the nitrogen as opposed to a fragmentation/recombination mechanism where the fluorine atom added is different from the one that is cleaved.

Neither restricted nor unrestricted CCSD(T) methods do well at describing biradical character. At the UCCSD(T)/cc-pVTZ//B3LYP/6-311+G(d) level, the enthalpy of the complex is 2.02 kcal/mol above F_2NO + F. When we projected out the effect of spin contamination from the DFT energies by an approximate method[39] (see Table 2) and referenced the enthalpy against the CCSD(T)/cc-VQZ value for F_2NO + F, the complex was 6.08 kcal/mol more stable than F_2NO + F radicals. Clearly, the relative enthalpies of the complex and F−F_2NO-ts are very uncertain. We feel that the enthalpies at the DFT level are too low, but that the enthalpies at UCCSD(T) are too high.

The electronic nature of the complex is an unsymmetrical two-center three-electron interaction (2c∴3e) between the unpaired electron on F and the lone pair on O ($F_2NO\therefore F$). The stability of this interaction is known to be exaggerated at the DFT level which is known to have excessive spin and charge delocalization.[40−43] Although a stabilization of 6.0 kcal/mol is probably too large, some stabilization is reasonable. Based on our results for the F + FNO complex (see below), we would expect F to bind to F_2NO with an enthalpy of 1−2 kcal/mol.

We decided to model the reaction of F_2NOF to F_3NO in two ways. The first model assumes that F_2NOF passes over F_2NO−F-ts in competition with fragmentation to F_2NO + F such that the intermediate and second transition state (F−F_2NO-ts) are unimportant. In other words, any species that cross the first barrier will form F_3NO. The second model is the same as the first except that the first transition state (F_2NO−F-ts) is assumed to lead to an intermediate and second transition state with the same energy. Thus, in the absence of reliable energies for the intermediate and second transition state, we assume the three structures have the same energy at 0K. In the second model, the intermediate can also fragment to F_2NO + F which will reduce the F_3NO product formation. In our calculations the branching ratio between the complex $\rightarrow F_3NO$ (k_7) and complex

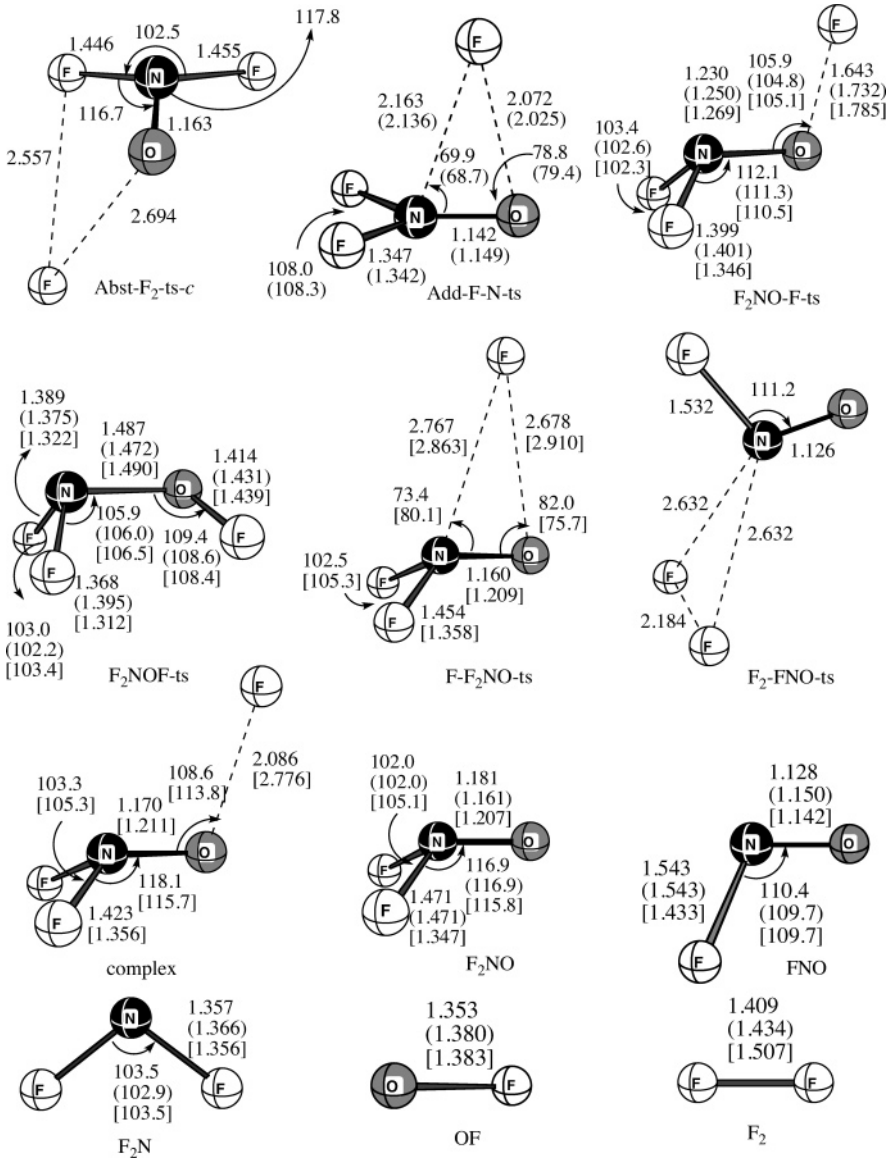

Figure 2. Optimized geometric parameters of stationary points at the B3LYP/6-311+G(d) level. Values in parentheses are at the CCSD/6-31+G-(d) level and values in brackets are at the CASSCF/6-311+G(d) level. Bond lengths are in Å and angles are in degrees.

$\rightarrow F_2NO + F$ (k_{11}) varied from 86:14 at 298 K to 67:33 at 1000 K (Table 7).

In comparing the first model, the rate of product formation is given by k_4, while in the second model, it is given by $k_9 = k_4k_7/(k_{-4}+k_7)$. Since $k_7 \gg k_{-4}$ (see Table 7), $k_4 \approx k_9$. However, the second model also includes fragmentation of the intermediate to $F_2NO + F$ which accounts for 7% of products at 298 K in our calculations.

Antoniotti et al.[1] found a transition state for the reaction *trans*-$F_2NOF \rightarrow F_3NO$ with a barrier of 22.2 kcal/mol at the CCSD-(T)/aug-cc-pVTZ//CCSD/cc-pVDZ level. In the present study, we find a zwitterionic transition state with a barrier of 23.06 kcal/mol (27.37−4.31, Table 2) which is very similar to the one found by Antoniotti et al. However, we also find a lower barrier of 9.79 kcal/mol through a biradical transition state (F_2-NO−F-ts). The relevant interactions between F and F_2NO in the two transition state are given in Figure 4. In the zwitterionic transition state (Add-F−N-ts, Figure 4a), the migrating F atoms have a large negative charge (0.61 e^-). The nitrogen center is planar in the F_2NO fragment as expected for $F_2N{=}O^+$. The fluoride sits above the N═O double bond and adds to the nitrogen side to form F_3NO. In the biradical transition state (F−F_2NO-ts, Figure 4b), the migrating F atom has little charge but large unpaired spin density (Table 3). The nitrogen center is pyramidal, as expected for a $F_2NO^{\bullet}$ radical. The reason for the large activation energy difference can be explained by the electronic excitation (Figure 4). The β-spin electron is excited from an a″ orbital to an a′ orbital which leaves an unpaired electron on nitrogen in an orbital which is suitable for bond formation with a fluorine atom. The energy needed for electronic excitation is the reason for the greater energy of Add-F−N-ts compared to F_2NO−F-ts.

The reaction of *trans*-$F_2NOF \rightarrow F_3NO$ can be considered a 1,2-fluorine shift which can be compared with the 1,2-hydrogen shift of NH_2OH. In their study of *trans*-$NH_2OH \rightarrow H_3NO$, Bach et al.[44] found a transition state with a 55.9 kcal/mol barrier at the MP4/6-31G(d)//MP2/6-31G(d) level, a barrier significantly lower than the H_2NO-H bond energy of 76.5 kcal/mol (Table 4). In the 1,2-fluorine shift, the barrier and F−O bond energies are nearly the same (Figure 3).

In their study of the $ClOONO \rightarrow ClONO_2$ reaction, Kovačič et al.[12] calculated an activation energy of 28 kcal/mol at the B3LYP/6-311G(d) level. The same reaction was found to have a much lower activation energy of 6.7 kcal/mol in a study in

TABLE 3: Spin Density, Natural Population Analysis (NPA), and Geometry Calculated at the (U)B3LYP/6-311+G(d)

		spin density			NPA charge			geometry		
	$\langle S^2 \rangle$	F	O	N	F	O	N	N−O	O−F	N−F
trans-F_2NOF	0.00	0.00	0.00	0.00	−0.11	0.01	0.56	1.38	1.43	2.21
F_2NO−F-ts	0.13	0.32	−0.12	−0.13	−0.18	−0.03	0.61	1.23	1.64	2.31
complex	0.81	0.82	−0.23	−0.41	−0.16	−0.14	0.70	1.17	2.08	2.69
F−F_2NO-ts	0.93	0.94	−0.29	−0.41	−0.05	−0.17	0.68	1.16	2.68	2.77
F_3NO	0.00	0.00	0.00	0.00	−0.22	−0.22	0.87	1.15	2.22	1.44
Add-F−N-ts	0.00	0.00	0.00	0.00	−0.61	−0.01	0.84	1.14	2.07	2.16

TABLE 4: Enthalpies and Free Energies of Fluorine Loss Reaction at the CCSD(T)/cc-pVQZ//B3LYP/6-311+G(d) Level

reaction	ΔH(298 K)	ΔG(298 K)	Dixon et al.	ΔH(0 K)[a]
cis-$F_2NOF \rightarrow F_2NO + F$	15.97	6.54	$H_2NOH \rightarrow H_2NO$+H	76.5
cis-$F_2NOF \rightarrow FNO + 2F$	20.54	2.56		
cis-$F_2NOF \rightarrow NO + 3F$	81.98	56.30		
$F_2NO \rightarrow FNO + F$	4.57	−3.98	$H_2NO \rightarrow HNO$+H	61.1
$FNO \rightarrow NO + F$	61.44	53.75	$HNO \rightarrow NO$+H	47.0

[a] Dixon, D. A.; Francisco, J. S.; Alexeev, Y. *J. Phys. Chem. A* **2006**, *110*, 185.

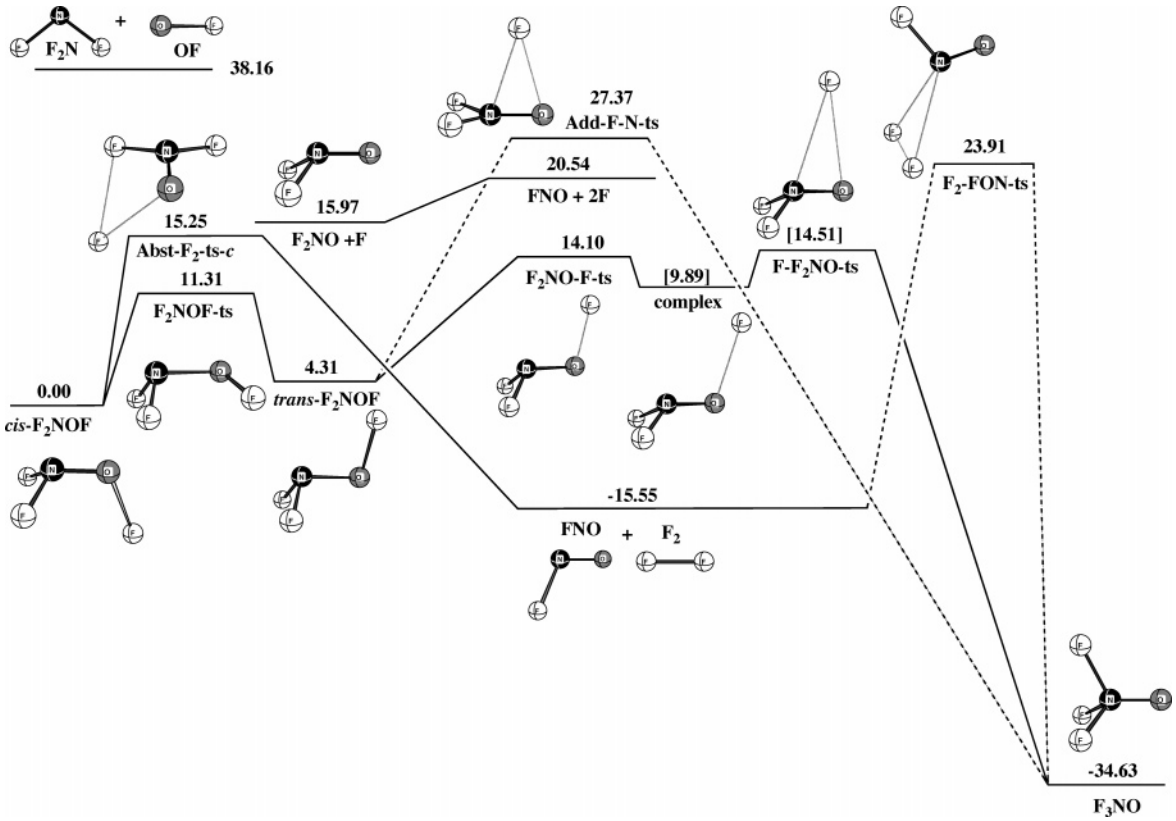

Figure 3. Schematic diagram of the potential energy surface for the dissociation of F_2NOF system computed at the CCSD(T)/cc-pVQZ//B3LYP/6-311+G(d) level. Relative enthalpies are given in kcal/mol at 298 K.

Zhu et al.[13] at the CCSD(T)/6-311+(3df)//B3LYP/6-311+G-(3df) level. The 6.7 kcal/mol barrier (0K) for the ClOONO → $ClONO_2$ reaction is much more consistent with our 9.79 kcal/mol barrier (298K) for the *trans*-$F_2NOF \rightarrow F_3NO$ reaction since the propensity for migrating a OCl radical should be similar to migrating a F radical.

The calculated bond enthalpy[45] at 298K for $ClO-NO_2$ (28.0 kcal/mol) and $BrO-NO_2$ (28.9 kcal/mol) at the CCSD(T) are in good agreement with experimental results (26.8 and 28.2 kcal/mol, respectively). We used the same method to find the FO−NF_2 bond enthalpy of 38.16 kcal/mol at the CCSD(T)/cc-pVQZ//B3LYP/6-311+G(d) level.

Stability of F_2NO. Breaking the weakest bond in *cis*-F_2NOF produces F_2NO + F radicals. The lifetime of a thermalized *cis*-F_2NOF molecule calculated from k_1 is 2.5×10^{-3} s at 298 K. However, the N−F bond enthalpy (298 K) is very small (4.57 and 3.57 kcal/mol at the CCSD(T)/cc-pVQZ//B3LYP/6-311+G-(d) and CCSD(T)/cc-pVQZ//CCSD/cc-pVDZ levels, respectively, Tables 4 and 5). In fact, the free energy change at 298 K is spontaneous (−3.98 kcal/mol) for breaking the N−F bond in F_2NO (Table 4). It is interesting that while the N−F bond in F_2NO is very weak, the N−F in FNO is very strong. Exactly the opposite behavior is calculated for the N−H bonds in H_2-NO and HNO where the first is 61.1 kcal/mol and the second one is 47.0 kcal/mol at 0K (Table 4). Fluorine is known to be a very good π donating substitutent. In FNO, fluorine can donate electron density into the π^* orbital of NO, whereas hydrogen cannot donate in HNO.

In contrast to F_2NOF and despite its lack of thermal stability, the difluoronitroxide radical (F_2NO) has been produced in solid argon matrixes by addition of F atoms to NO by Misochko et al.[7] They found that F_2NO exists in equilibrium (F−FNO ⇄

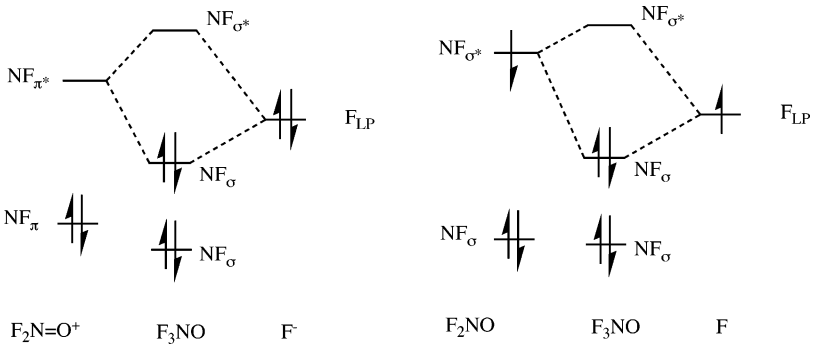

Figure 4. Interaction diagram comparing (a) the zwitterionic tansition state (Add-F−N-ts) and (b) the biradical transtion state (F−F_2NO-ts).

TABLE 5: Enthalpies of the Various Types of F_2NO Species Optimized at the CCSD/cc-pVDZ Level

	Δ*H*(0 K)			Δ*H*(298 K)		
	CCSD/cc-pVDZ	CCSD(T)/cc-pVTZ	CCSD(T)/cc-pVQZ	CCSD/cc-pVDZ	CCSD(T)/cc-pVTZ	CCSD(T)/cc-pVQZ
F_2NO[a]	0.00	0.00(0.00)	0.00(0.00)	0.00	0.00(0.00)	0.00(0.00)
t-F−FNO-c_s[a]	−6.95	1.24(1.35)	2.79(2.86)	−5.73	2.46(2.57)	4.01(4.08)
c-F−FNO-c_s	−6.89	1.16	2.75	−5.71	2.34	3.93
F−FNO-ts	3.38	5.67	5.66	3.44	5.75	5.74
FNO+F	−5.88	2.05(1.95)	3.57(3.44)	−4.75	3.18(3.01)	4.70(4.51)

[a] The data in the parentheses are at CCSD(T)/cc-pVDZ optimized geometries.

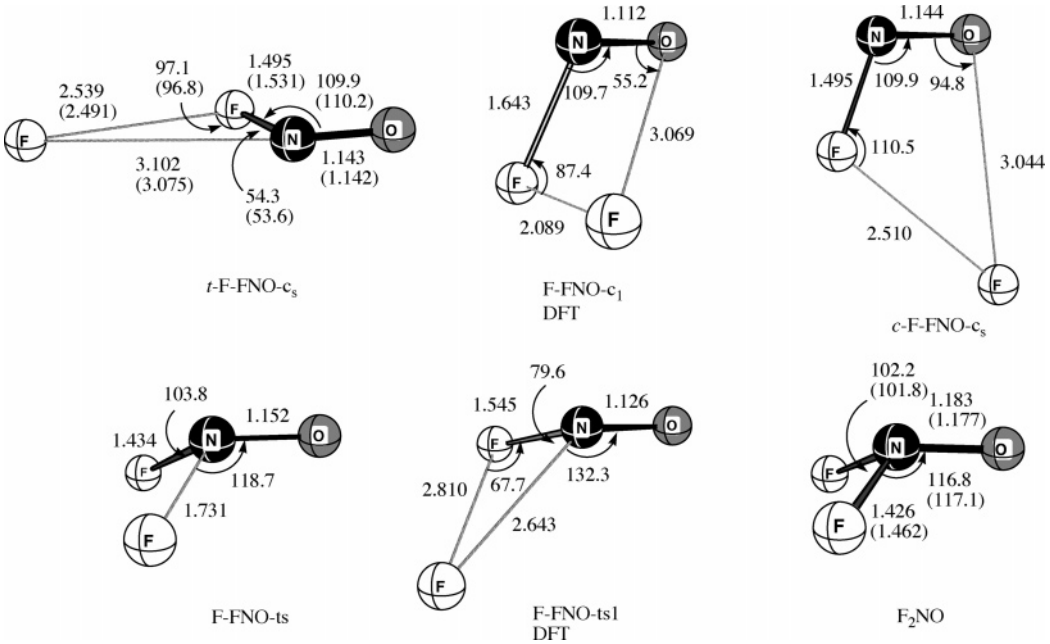

Figure 5. Optimized geometric parameters of stationary points at the CCSD/cc-pVDZ level. The parameters in parentheses are optimized at the CCSD(T)/cc-pVDZ level. The values for F−FNO-c_1 and F−FNO-ts_1 are at the B3LYP/6-311G(d) level.

F_2NO) with a van der Waals complex (F−FNO). Since F_2NO and the complex were formed at very low temperature (20 K), we compared our results at 0 K with experimental results at Table 5. The reaction mechanism of $F_2NO \rightarrow FNO + F$ are calculated at the CCSD(T)/cc-pVQZ//CCSD/cc-pVDZ. The complex (F−FNO) and transition state (F−FNO-ts) are located at the CCSD/cc-pVDZ level. The optimized geometries of the complex and transition state at the B3LYP/6-311+G(d) level are compared with CCSD/cc-pVDZ in Figure 5. The CCSD-(T)/cc-pVDZ method was used to optimize geometries for the complex (*t*-F−FNO-c_s) and F_2NO and found to give very similar geometries with the CCSD/cc-pVDZ method. While B3LYP gives reasonable structures for halogen compounds, it is interesting that B3LYP failed for the complex. The reason for this can be understood by excessive spin delocalization in DFT that is a particular problem in asymmetric 2c-3e bonding[40−43] (Table 6).

TABLE 6: Spin Densities and Mulliken Charges for c−F−FNO-c_s and F−FNO-c_1

	CCSD/cc-pVDZ// CCSD/cc-pVDZ		B3LYP/6-311+G(d)// B3LYP/6-311+G(d)	
	c-F−FNO-c_s		F−FNO-c_1	
	spin density	Mulliken charges	spin density	Mulliken charges
O	0.00	0.00	−0.02	0.24
N	0.00	0.29	−0.00	0.06
F	0.01	−0.28	0.17	−0.18
F	0.99	−0.01	0.85	−0.12

We optimized two F−FNO complexes at the CCSD/cc-pVDZ level (*c*-F−FNO-c_s and *t*-F−FNO-c_s, Table 5) and one at the CCSD(T)/cc-pVDZ level (*t*-F−FNO-c_s). The cis complex is very slightly more stable (by 0.04 kcal/mol at 0 K), but the trans complex should be formed first by the principle of least motion. Both cis and trans complexes are very different from the

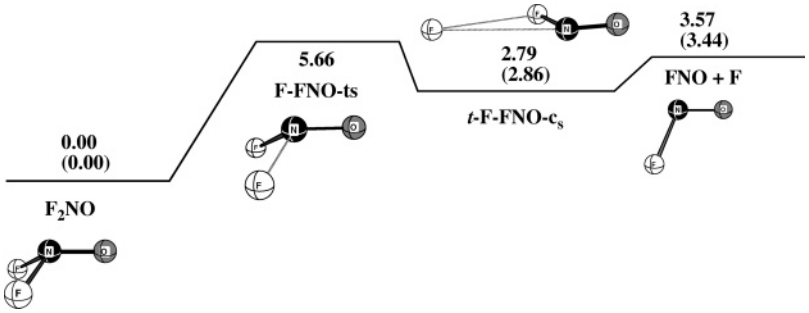

Figure 6. Schematic diagram of the potential energy surface $\Delta H(0\ \mathrm{K})$ for the dissociation of F_2NO at the CCSD(T)/cc-pVQZ//CCSD/cc-pVDZ level. Values in parentheses are at the CCSD(T)/cc-pVQZ//CCSD(T)/cc-pVDZ level.

complex obtained at the DFT level (Figure 5). In the radical complex between FNO and F at the DFT level, the interaction is between the unpaired electron on one fluorine and the lone pair of another fluorine. The oxygen lone pair electrons in FNO have been stabilized (relative to F_2NO) which leads to a stronger interaction with the lone pairs on F of FNO.

We calculated $\Delta H° = -2.75$ kcal/mol enthalpy and $\Delta S° = -13.76$ cal/mol·K entropy for the reaction F−FNO $\rightleftarrows$ F_2NO at 0 K (Table 5). Experimental results show that the changes in enthalpy and entropy at 20 K for the equilibrium reaction (F−FNO $\rightleftarrows$ F_2NO) are 0.29 kcal/mol and 14.82 cal/mol·K, respectively. However, it is not possible to make a direct comparison between experiment and theory because the calculations model the gas phase, whereas the experiment takes place in an Ar matrix. A greater stabilization energy for the complex could be rationalized by greater dipole−induced dipole interactions between Ar molecules and the complex, since the complex has a higher dipole moment than F_2NO (1.548 and 0.413 D, respectively) at the CCSD/cc-pVDZ level and dipole−induced dipole interactions are directly proportional to the dipole moment. The lifetime for F_2NO is only 2.69×10^{-10} s^{-1} at 298 K from k_8.

Rate Constant Calculations. Since there is no reverse barrier for *cis*-$F_2NOF \rightarrow F_2NO + F$ (k_1) and *trans*-$F_2NOF \rightarrow F_2NO + F$ (k_5), we used Variflex to calculate the rate constants (see eqs 7−10). The reactive flux was evaluated by the phase-space-integral based VTST (PSI−VTST) method, as implemented in VariFlex[34] as the O−F distances increased from 1.5 to 4.0 Å with a step size 0.1 Å for *cis*-$F_2NOF \rightarrow F_2NO + F$ and *trans*-$F_2NOF \rightarrow F_2NO + F$ reactions.

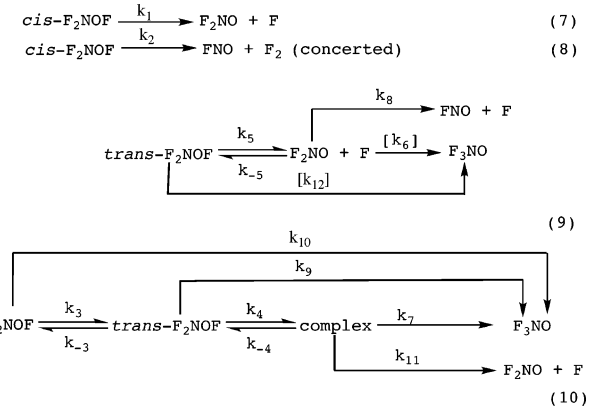

Chemrate was used to calculate the isomerization (*cis*-F_2NOF $\rightleftarrows$ *trans*-F_2NOF) rate constants (k_3, k_{-3}). Chemrate includes a master equation solver so that rate constants for unimolecular reactions can be determined on the basis of RRKM theory in the energy transfer region and chemical activation processes under steady and non-steady conditions. CCSD(T)/cc-pVQZ//B3LYP/6-311+G(d) energies are used with B3LYP/6-311+G(d) optimized geometries and thermal corrections in Chemrate.

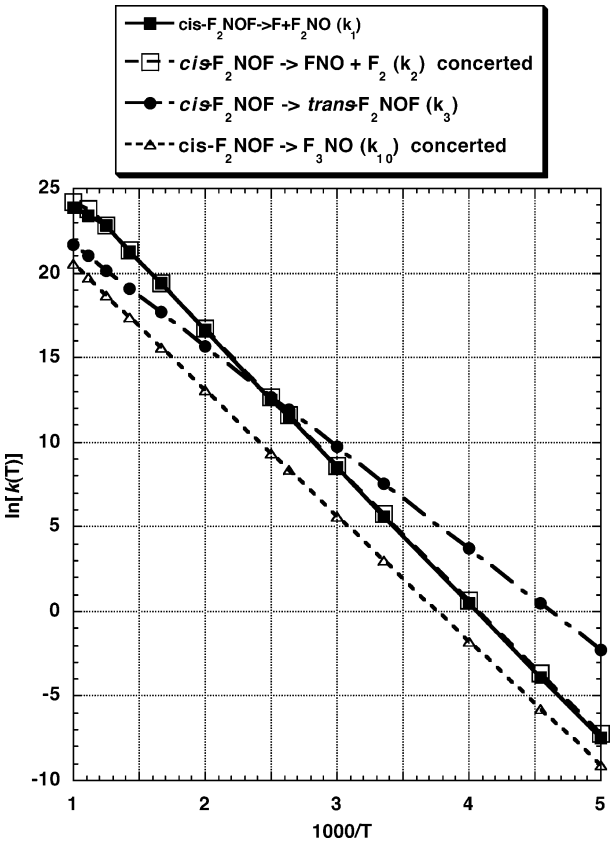

Figure 7. Calculated rate constants involving *cis*-F_2NOF. The computational rate data are for the unimolecular rate constant at the high-pressure limit.

Figure 7 compares the calculated rate constants (high-pressure limit) for production of $F_2NO + F$ (k_1) and $FNO + F_2$ (k_2). Since TST rate constants and VTST rate constants are similar for *cis*-$F_2NOF \rightarrow FNO + F_2$ (concerted) as the temperature decreases, variational effect can be ignored for this reaction. The rate constant for *cis*-$F_2NOF \rightarrow F_2NO + F$ and *cis*-$F_2NOF \rightarrow FNO + F_2$ are calculated as $k_1 = 6.37 \times 10^{13} \exp(-7855/T)$ and $k_2 = 8.14 \times 10^{13} \exp(-7860/T)$, respectively.

The rate constant for formation of F_3NO is derived with a steady-state approximation [$k_{10} = k_3k_4k_7/(k_{-3}(k_{-4} + k_7))$] via *trans*-$F_2NOF$ in eq 10. Since the F_2NO−F-ts transition state is calculated with an accurate method (RCCSD(T)/cc-pVQZ//UB3LYP/6-311+G(d)), we used this transition state to calculate a rate constant of $1.42 \times 10^{12} \exp(-7420/T)$ for k_{10}.

We also checked our rate constant result corresponding to eq 10 with a steady-state approximation for the complex [$k_9 =$

TABLE 7: Rate Constant with Temperature Dependence at High-Pressure Limit for Formation of F_3NO and Dissociation of Complex to Radicals

temp (K)	k_4	k_{-4}	k_7	k_{11}
200	4.45×10	1.04×10^{12}	1.09×10^{14}	2.03×10^{12}
220	4.68×10^{2}	1.01×10^{12}	1.01×10^{14}	2.71×10^{12}
250	7.95×10^{3}	9.78×10^{11}	9.22×10^{13}	3.87×10^{12}
298	2.28×10^{5}	9.29×10^{11}	8.40×10^{13}	5.95×10^{12}
333	1.46×10^{6}	8.99×10^{11}	8.02×10^{13}	7.60×10^{12}
380	1.01×10^{7}	8.66×10^{11}	7.69×10^{13}	9.85×10^{12}
400	2.03×10^{7}	8.54×10^{11}	7.58×10^{13}	1.08×10^{13}
500	2.83×10^{8}	8.05×10^{11}	7.23×10^{13}	1.56×10^{13}
600	1.65×10^{9}	7.74×10^{11}	7.05×10^{13}	2.00×10^{13}
700	5.83×10^{9}	7.52×10^{11}	6.94×10^{13}	2.40×10^{13}
800	1.51×10^{10}	7.37×10^{11}	6.87×10^{13}	2.76×10^{13}
900	3.15×10^{10}	7.26×10^{11}	6.83×10^{13}	3.07×10^{13}
1000	5.69×10^{10}	7.18×10^{11}	6.80×10^{13}	3.35×10^{13}

$k_4k_7/(k_{-4} + k_7)$]. Since the complex and F_2−NOF-ts could not be calculated accurately due to spin contamination, we assume that complex and F−F_2NOF-ts have the same energy as F_2-NO−F-ts in the rate constant calculations. Rate constants k_{-4} and k_7 are calculated by Polyrate and k_8 is calculated by Variflex. Since k_{-4} is small and k_7 is large ($k_7 \gg k_{-4}$), the overall rate becomes $k_9 \approx k_4$. We also include the possibility of dissociation of the complex (k_8) to radicals ($F_2NO + F$) in the rate constant for F_3NO formation. Table 7 shows that k_7 is 14 times faster than the rate constant of complex dissociation to radicals (k_{11}) at room temperature which will reduce the formation of F_3NO seven percent at room temperature.

At all temperatures, the ratio of $F_2NO + F$ (k_1) formation to $FNO + F_2$ (k_2) is very similar but much faster than F_3NO formation. Since F_2NO has a very short lifetime, it can quickly dissociate to FNO + F. Depending on the rate of 2F radical−radical recombination, the dominant products from F_2NOF decomposition are expected to be FNO, F_2, and F. It is interesting to note that Fox et al.[14] suggested that the observed formation of F_3NO from the reaction of F_2 plus NO in a 2000 K flame probably involved an excited-state intermediate.

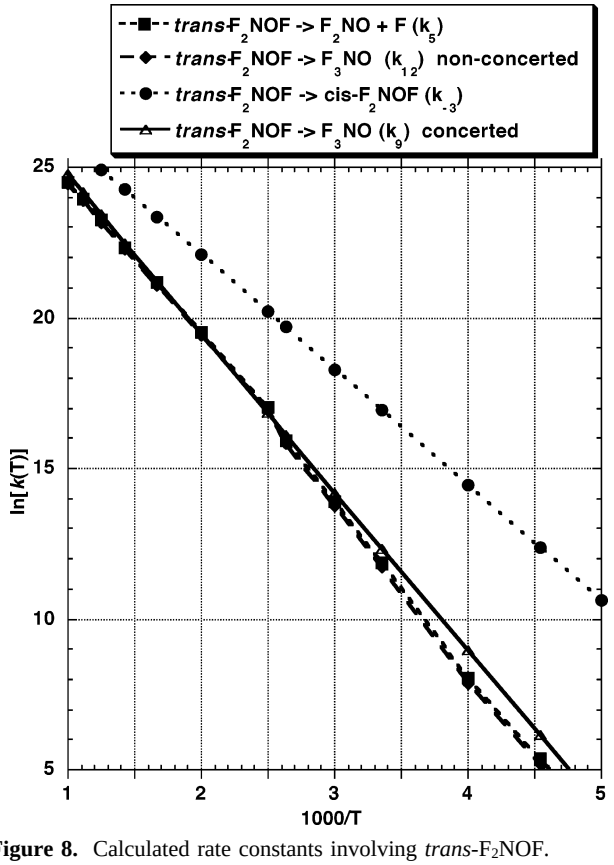

Figure 8. Calculated rate constants involving *trans*-F_2NOF.

Although the addition of F to F_2NO does not play a role in F_3NO formation,[46] we compared this path (nonconcerted path, k_{12}) with the concerted path (k_9) of *trans*-$F_2NOF \rightarrow F_3NO$ that can be formed with activation enthalpy 14.10 kcal/mol. Our calculated results show that the concerted path (k_9) is faster than the nonconcerted path (k_{12}) for *trans*-$F_2NOF \rightarrow F_3NO$ at low temperatures (Figure 8). This result may have implications in reactions where the radicals generated have longer lifetimes, such as in the $FONO \rightarrow FNO_2$ rearrangement. In that reaction, a radical/radical complex may lead to a concerted/nonconcerted branching ratio.

Conclusion

Perfluorohydroxylamine (F_2NOF) is a challenging molecule for theory and its short lifetime suggests that it will be a challenge for experiment as well. The O−F bond enthalpy (298K) is calculated at the CCSD(T)/cc-pVQZ//B3LYP/6-311+G(d) level to be 15.97 kcal/mol. In competition with O−F bond fragmentation, *cis*-F_2NOF can eliminate F_2 or isomerize to *trans*-F_2NOF. In turn, trans-F_2NOF can cleave the O−F bond or rearrange to F_3NO via an intermediate $F + F_2NO$ complex. Rate constants have been calculated for the different pathways in order to determine the products formed. At room temperature, only 3% of products $k_{10}/(k_1+k_2+k_{10})$ is expected to be F_3NO even though it is the global minimum.

Acknowledgment. Computer time was made available on the Alabama Supercomputer Network. We thank Dr. Thomas Webb for helpful conversations.

Supporting Information Available: B3LYP/6-311+G(d) and CCSD(T)/cc-pVTZ//B3LYP/6-311+G(d), CCSD(T)/cc-pVQZ//B3LYP/6-311+G(d) energies (hartrees), zero-point energies (kcal/mol), heat capacity corrections to 298 K (kcal/mol), and entropies (cal/mol·K) at the B3LYP/6-311+G(d) level are tabulated in Table S1. Total energies, zero-point energies (kcal/mol), heat capacity corrections to 298 K (kcal/mol), and entropies (cal/mol·K) at the CCSD/cc-pVDZ level are tabulated in Table S2 for F_2NO species. Rate constants are given in Table S3 for k_1−k_6 and k_8 and Table S4 for k_9, k_{10}, and k_{12}. Total and relative energies at CASSCF optimized geometries are given in Table S5. Cartesian coordinates of all optimized structures at the B3LYP/6-311+G(d) level (and several at UB3LYP/6-311+G(d) level) are given in Table S6. This material is available free of charge via the Internet at http://pubs.acs.org.

References and Notes

(1) Antoniotti, P.; Grandinetti, F. *Chem. Phys. Lett.* **2002**, *366*, 676.
(2) Erben, M. F.; Diez, R. P.; Védova, C. O. D. *Chem. Phys.* **2005**, *308*, 193.
(3) Dewar, M. J. S.; Rzepa, H. S. *J. Am. Chem. Soc.* **1978**, *100*, 58.
(4) (a) Olsen, J. F.; Howell, J. M. *J. Fluorine Chem.* **1978**, *12*, 123. (b) Olsen, J. F.; O'Connor, D.; Howell, J. M. *J. Fluorine Chem.* **1978**, *12*, 179.
(5) Plato, V.; Hartford, W. D.; Hedberg, K. *J. Chem. Phys.* **1970**, *53*, 3488.
(6) Bedzhanyan, Yu. R.; Gershenzon, Yu. M.; Rozenshtein, V. B. *Kinet. Katal.* **1990**, *31*, 1474.
(7) (a) Misochko, E. Ya.; Akimov, A. V.; Goldschleger, I. U. *J. Am. Chem. Soc.* **1998**, *120*, 11520. (b) Misochko, Yu. R.; Akimov, A. V.; Goldschleger, I. U.; Boldyrev, A. I.; Wight, C. A. *J. Am. Chem. Soc.* **1999**, *121*, 405.
(8) Ellison, G. B.; Herbert, J. M.; McCoy, A. B.; Stanton, J. F.; Szalay, P. G. *J. Phys. Chem. A* **2004**, *108*, 7639.
(9) Sayin, H.; McKee, M. L. *J. Phys. Chem. A* **2005**, *109*, 4736.

(10) Kovačič, S.; Lesar, A.; Hodošček, M. *Chem. Phys. Lett.* **2005**, *413*, 36.

(11) (a) Zhao, Y.; Houk, K. N.; Olson, L. P. *J. Phys. Chem. A* **2004**, *108*, 5864. (b) Zhang, J.; Donahue, N. M. *J. Phys. Chem. A* **2006**, *110*, 6898. (c) Srinivasan, N. K.; Su, M.-C.; Sutherland, J. W.; Michael, J. V.; Ruscic, B. *J. Phys. Chem. A* **2006**, *110*, 6602. (d) Hippler, H.; Krasteva, N.; Nasterlack, S.; Striebel, F. *J. Phys. Chem. A* **2006**, *110*, 6781.

(12) Kovačič, S.; Lesar, A.; Hodošček, M. *J. Chem. Inf. Model.* **2005**, *45*, 58.

(13) Zhu, R. S.; Lin, M. C. *Chem. Phys. Chem.* **2005**, *6*, 1514.

(14) Fox, W. B.; Sukornick, B.; Mackenzie, J. S.; Sturtevant, R. L.; Maxwell, A. F.; Holmes, J. R. *J. Am. Chem. Soc.* **1970**, *92*, 5240.

(15) Lee, T. J.; Bauschlicher, C. W., Jr.; Jayatilaka, D. *Theor. Chem. Acc.* **1997**, *97*, 185.

(16) Guha, S.; Francisco, J. S. *J. Phys. Chem. A* **1997**, *101*, 5347.

(17) Francisco, J. S.; Clark, J. *J. Phys. Chem. A* **1998**, *102*, 2209.

(18) Parthiban, S.; Lee, T. J. *J. Chem. Phys.* **2000**, *113*, 145.

(19) Zhao, Y.; Lynch, B. J.; Truhlar, D. G. *J. Phys. Chem. A* **2004**, *108*, 2715.

(20) Zhao, Y.; Truhlar, D. G. *J. Phys. Chem. A* **2004**, *108*, 6908.

(21) Hehre, W. J.; Radom, L.; Schleyer, P. v. R.; Pople, J. A. *Ab initio Molecular Orbital Theory*; Wiley: New York, 1987.

(22) Lynch, B. J.; Zhao, Y.; Truhlar, D. G. *J. Phys. Chem. A* **2003**, *107*, 1384.

(23) Lee, T. J.; Scuseria, G. E. *J. Chem. Phys.* **1990**, *93*, 489.

(24) Scuseria, G. E. *J. Chem. Phys.* **1991**, *94*, 442.

(25) Frisch, M. J.; Trucks, G. W.; Schlegel, H. B.; Scuseria, G. E.; Robb, M. A.; Cheeseman, J. R.; Montgomery, J. A., Jr.; Vreven, T.; Kudin, K. N.; Burant, J. C.; Millam, J. M.; Iyengar, S. S.; Tomasi, J.; Barone, V.; Mennucci, B.; Cossi, M.; Scalmani, G.; Rega, N.; Petersson, G. A.; Nakatsuji, H.; Hada, M.; Ehara, M.; Toyota, K.; Fukuda, R.; Hasegawa, J.; Ishida, M.; Nakajima, T.; Honda, Y.; Kitao, O.; Nakai, H.; Klene, M.; Li, X.; Knox, J. E.; Hratchian, H. P.; Cross, J. B.; Bakken, V.; Adamo, C.; Jaramillo, J.; Gomperts, R.; Stratmann, R. E.; Yazyev, O.; Austin, A. J.; Cammi, R.; Pomelli, C.; Ochterski, J. W.; Ayala, P. Y.; Morokuma, K.; Voth, G. A.; Salvador, P.; Dannenberg, J. J.; Zakrzewski, V. G.; Dapprich, S.; Daniels, A. D.; Strain, M. C.; Farkas, O.; Malick, D. K.; Rabuck, A. D.; Raghavachari, K.; Foresman, J. B.; Ortiz, J. V.; Cui, Q.; Baboul, A. G.; Clifford, S.; Cioslowski, J.; Stefanov, B. B.; Liu, G.; Liashenko, A.; Piskorz, P.; Komaromi, I.; Martin, R. L.; Fox, D. J.; Keith, T.; Al-Laham, M. A.; Peng, C. Y.; Nanayakkara, A.; Challacombe, M.; Gill, P. M. W.; Johnson, B.; Chen, W.; Wong, M. W.; Gonzalez, C.; Pople, J. A. *Gaussian 03*, revision B.4; Gaussian, Inc.: Wallingford, CT, 2004.

(26) Schmidt, M. W.; Baldridge, K. K.; Boatz, J. A.; Elbert, S. T.; Gordon, M. S.; Jensen, J. H.; Koseki, S.; Matsunaga, N.; Nguyen, K. A.; Su, S.; Windus, T. L.; Dupuis, M.; Montgomery, J. A. *J. Comput. Chem.* **1993**, *14*, 1347.

(27) Schaftenaar, G.; Noordik, J. H. *J. Comput.-Aided Mol. Des.* **2000**, *14*, 123.

(28) Roos, B. O. The complete active space self-consistent field method and its applications in electronic structure calculations. Lawley, K. P., Ed.; In *Advances in Chemical Physics; Ab Initio Methods in Quantum Chemistry-II*; John Wiley & Sons: Chichester, U.K., 1987.

(29) Nakano, H. *J. Chem. Phys.* **1993**, *99*, 7983.

(30) Gonzalez, C.; Schlegel, H. B. *J. Phys. Chem.* **1989**, *93*, 2154.

(31) Garrett, B. C.; Truhlar, D. G. *J. Chem. Phys.* **1984**, *81*, 309.

(32) Truhlar, D. G.; Garrett, B. C.; Klippenstein, S. J. *J. Phys. Chem.* **1996**, *100*, 12771.

(33) Chuang, Y.-Y.; Corchado, J. C.; Truhlar, D. G. *J. Phys. Chem. A* **1999**, *103*, 1140.

(34) Klippenstein, S. J.; Wagner, A. F.; Dunbar, R. C.; Wardlaw, D. M.; Robertson, S. H. *VariFlex*, version 1.00; Argonne National Laboratory: Argonne, IL, 1999.

(35) Mokrushin, V.; Bedanov, V.; Tsang, W.; Zachariah, M. R.; Knyazev, V. D. *ChemRate*, version 1.21; National Institute of Standards and Technology: Gaithersburg, MD, 2002.

(36) Corchado, J. C.; Chuang, Y.-Y.; Fast, P. L.; Villa, J.; Hu, W.-P.; Liu, Y.-P.; Lynch, G. C.; Nguyen, K. A.; Jackels, C. F.; Melissas, V. S.; Lynch, I. R.; Coitino, E. L.; Fernandez-Ramos, A.; Pu, J.; Albu, T. V.; Steckler, R.; Garrett, B. C.; Isaacson, A. D.; Truhlar, D. G. *Polyrate*, version 9.3; University of Minnesota: MN, 2004.

(37) Dunning-type basis sets (a) cc-pVDZ: Woon, D. E.; Dunning, T. H. *J. Chem. Phys.* **1993**, *98*, 1358. (b) cc-pVTZ: Kendall, R. A.; Dunning, T. H.; Harrison, R. J. *J. Chem. Phys.* **1992**, *96*, 6796. (c) cc-pVQZ: Dunning T, H. *J. Chem. Phys.* **1989**, *90*, 1007.

(38) When calculating the rate constant using VTST, the energy of the points along the IRC at the UCCSD(T)/cc-pVTZ level were shifted upward by 0.72 kcal/mol to be consistent with the correction for the Abst-F_2-ts-*c* transition state.

(39) (a) Noodleman, L.; Case, D. A. *Adv. Inorg. Chem.* **1992**, *38*, 423. (b) See: Bally, T.; Borden, W. T. In *Reviews in Computational Chemistry*; Lipkowitz, K. B., Boyd, D. B., Eds.; Wiley: New York, 1999; Vol. 13, p 1.

(40) Fourré, I.; Silvi, B.; Sevin, A.; Chevreau, H. *J. Phys. Chem. A* **2002**, *106*, 2561.

(41) Braïda, B.; Thogersen, L.; Wu, W.; Hiberty, P. C. *J. Am. Chem. Soc.* **2002**, *124*, 11781.

(42) Braïda, B.; Hiberty, P. C. *J. Phys. Chem. A* **2000**, *104*, 4618.

(43) Braïda, B.; Hiberty, P. C.; Savin, A. *J. Phys. Chem. A* **1998**, *102*, 7872.

(44) Bach, R. D.; Owensby, A. L.; Gonzalez, C.; Schlegel, H. B.; McDouall, J. J. W. *J. Am. Chem. Soc.* **1991**, *113*, 6001.

(45) Zou, P.; Derecskei-Kovacs, A.; North, S. W. *J. Phys. Chem. A* **2003**, *107*, 888.

(46) If we compare k_8/[F] and k_6 at 298 K where [F] is assumed to be 0.01 atm, then the unimolecular rate (k_8[F_2NO]) is still 2300 times faster than the bilmolecular rate (k_6[F_2NO][F]).